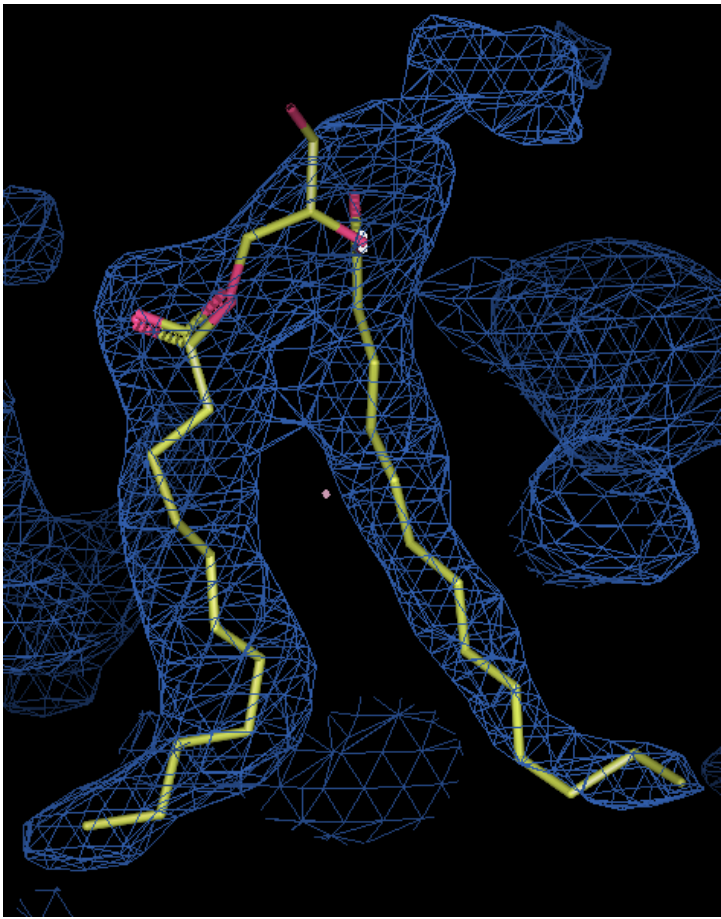
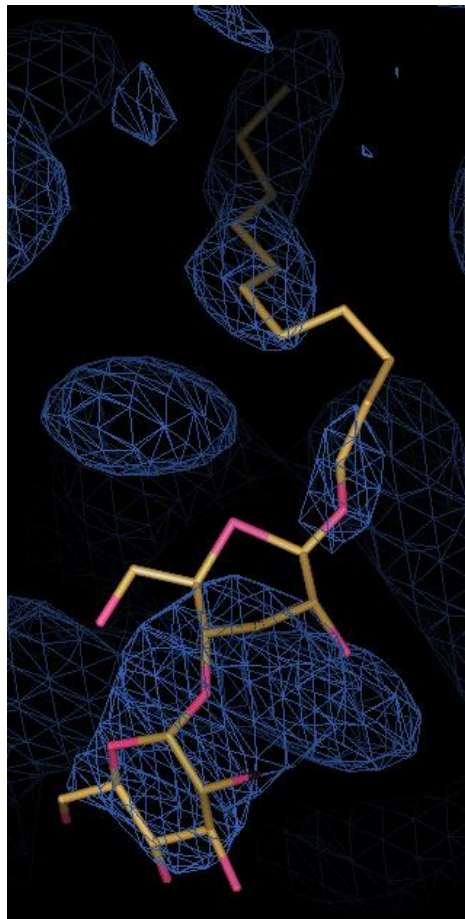


Figure S1

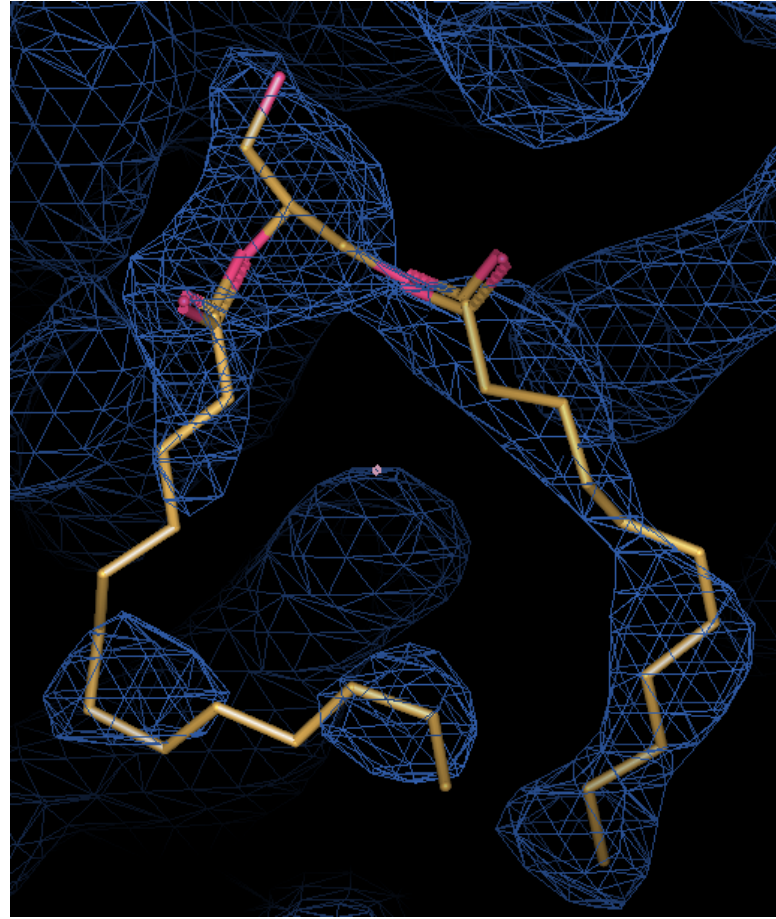
A. DAG6



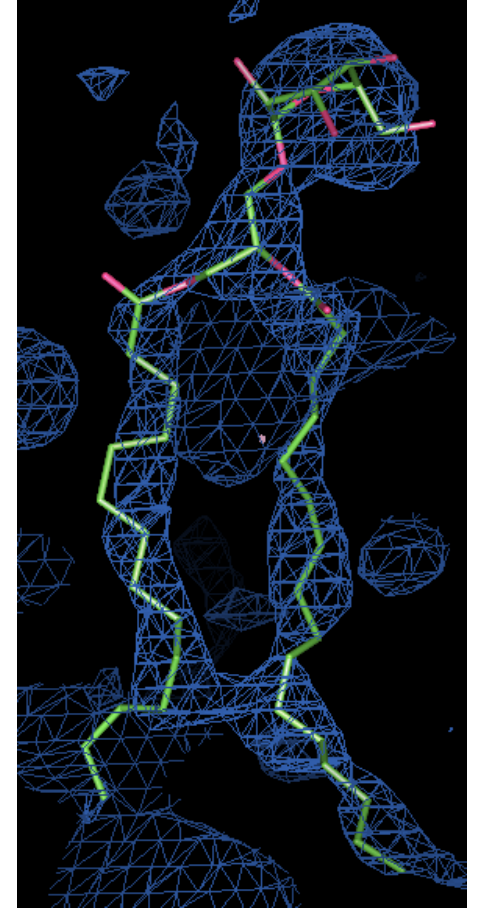
B. UDM2



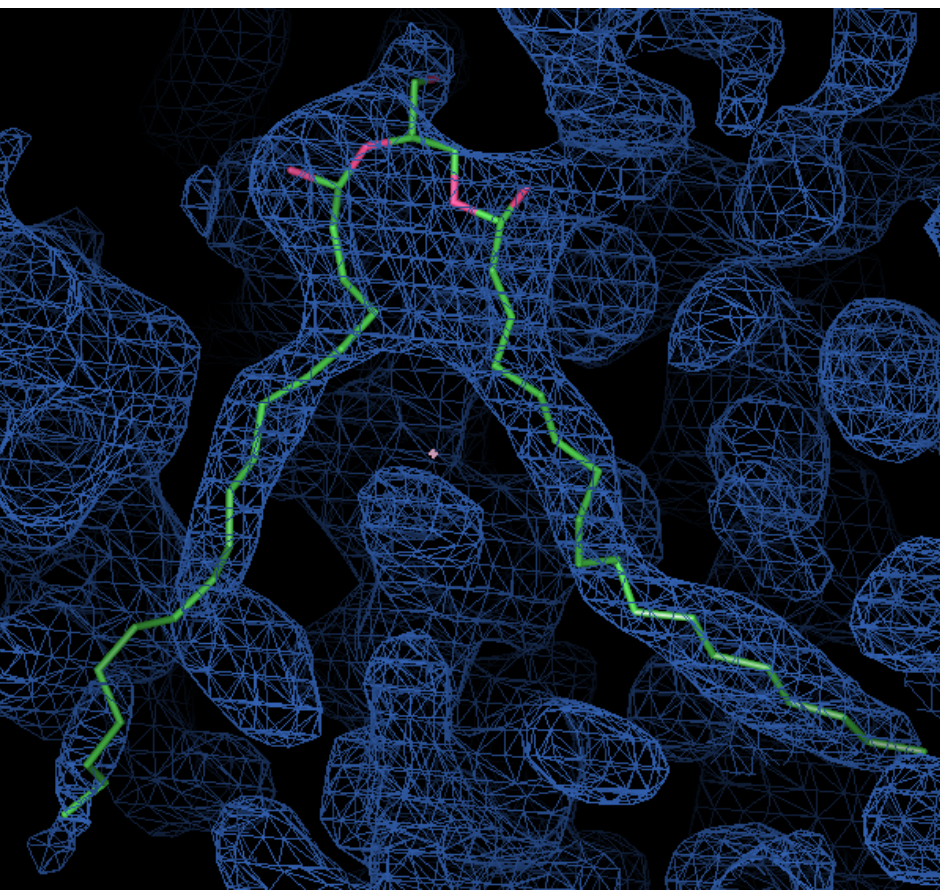
C. DAG7



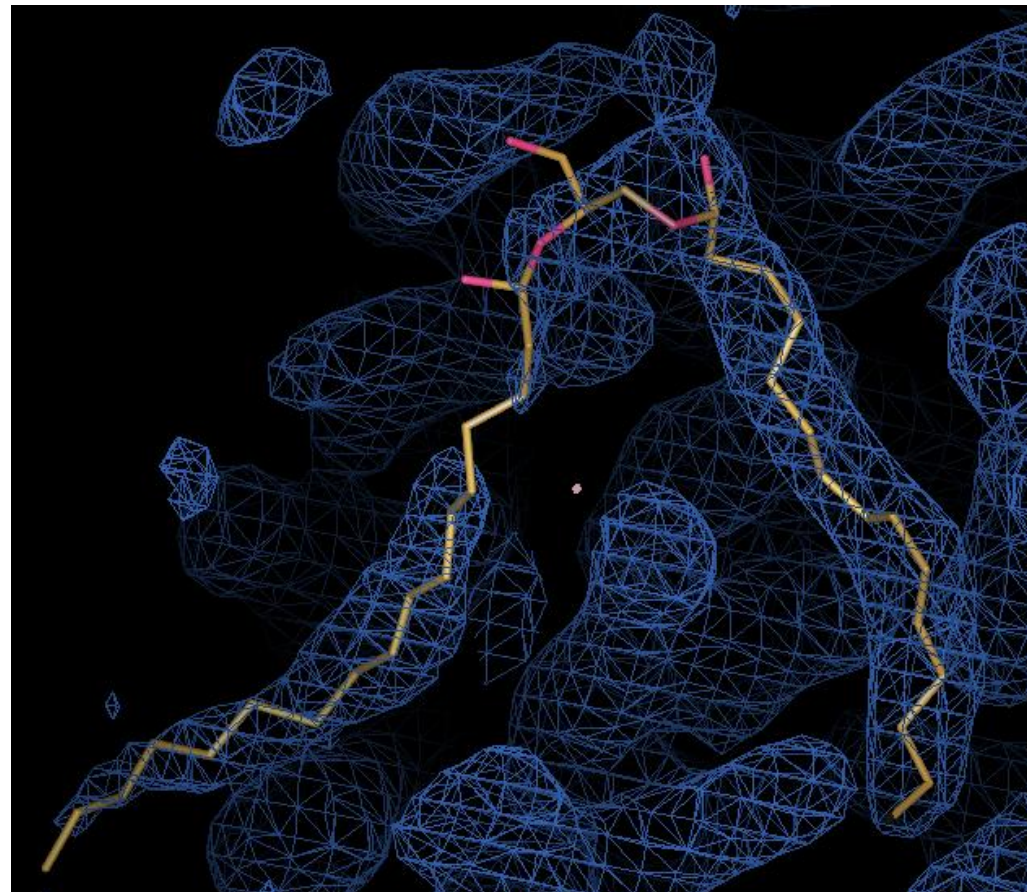
D. MGDG



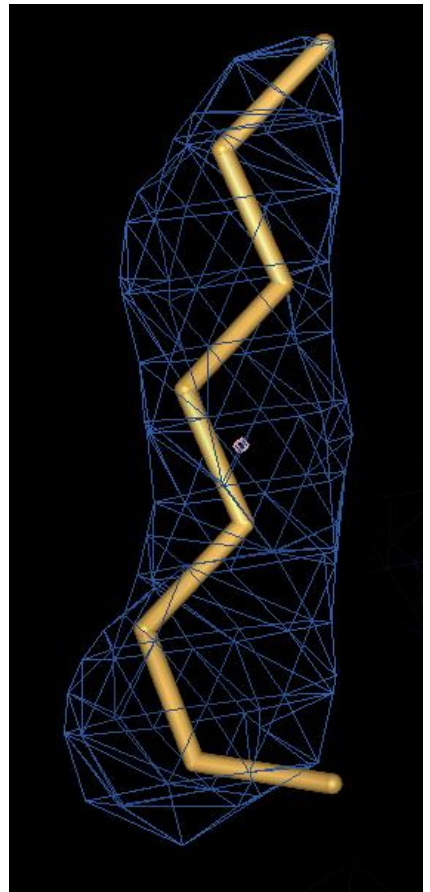
E. DAG4



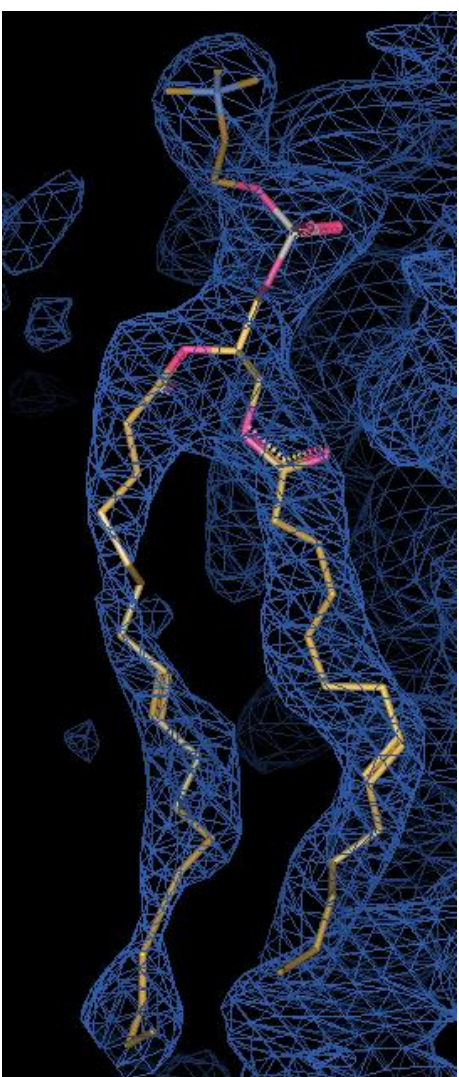
F. DAG5



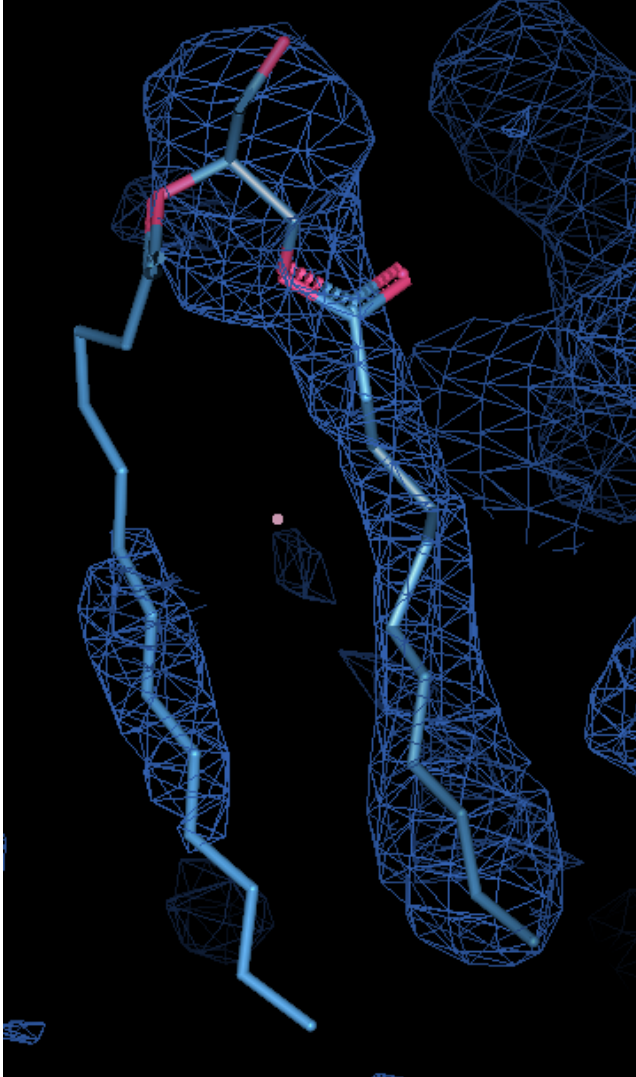
G. OCT



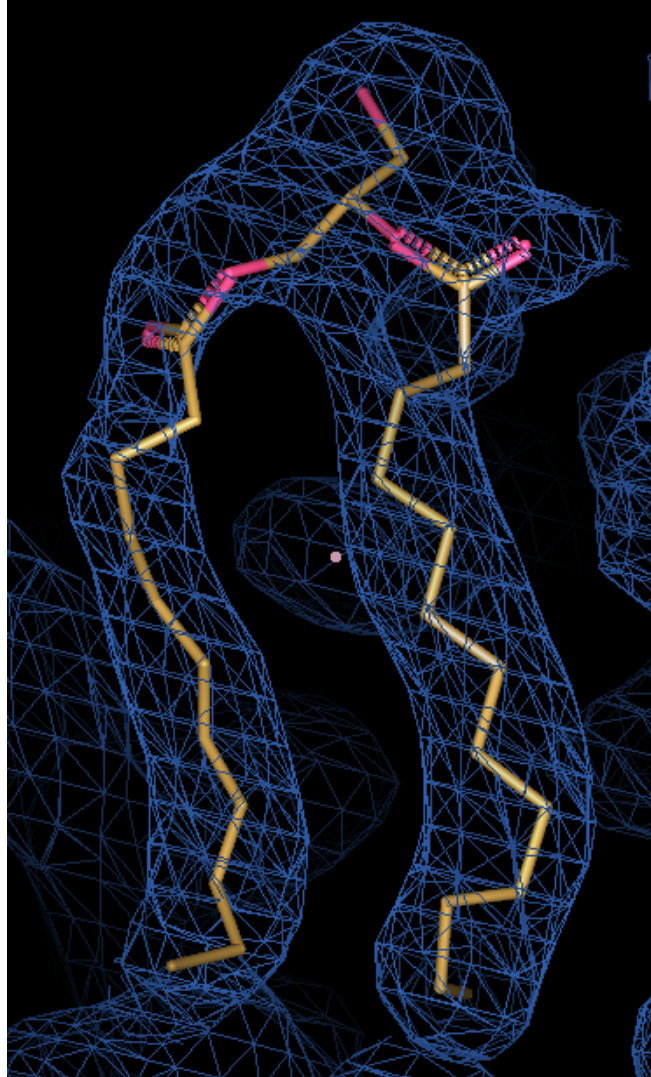
H. DOPC



I. DAG8



J. DAG2



K. DAG1

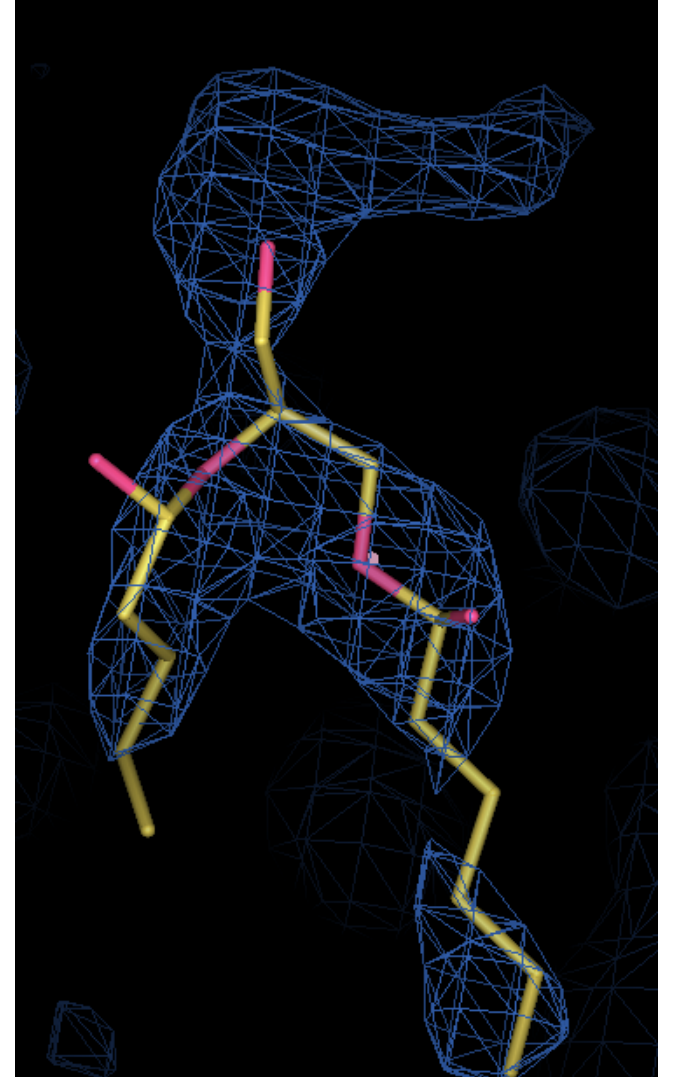
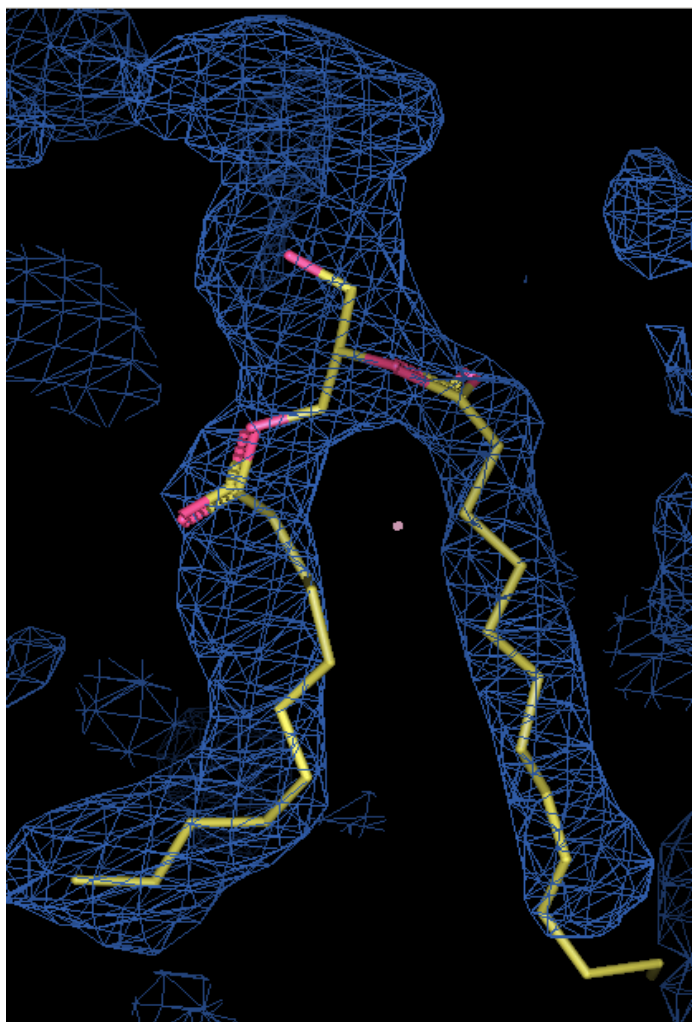
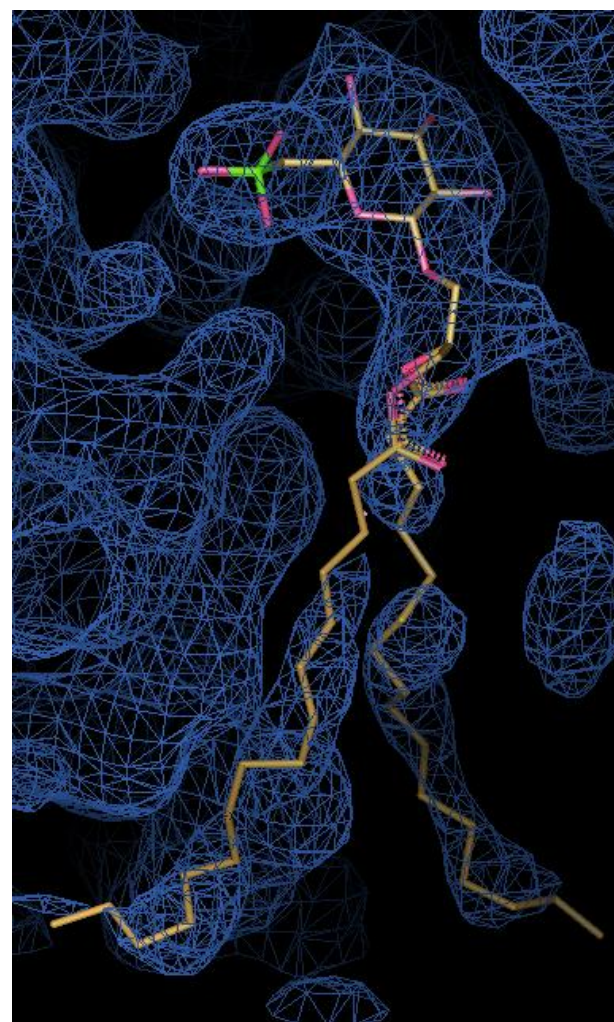


Figure S1

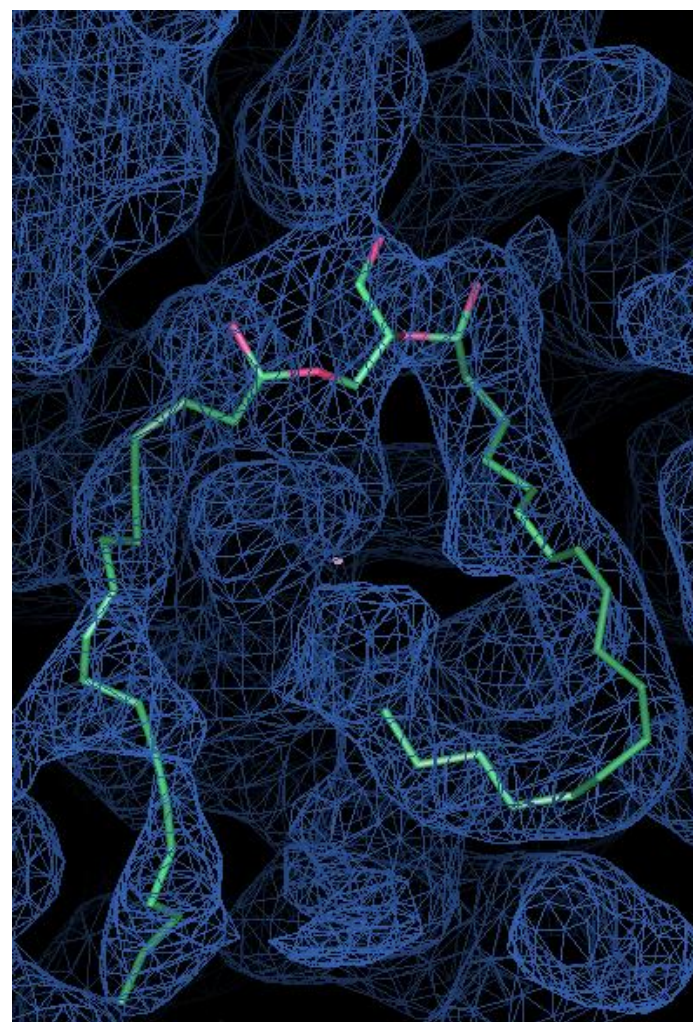
L. DAG3



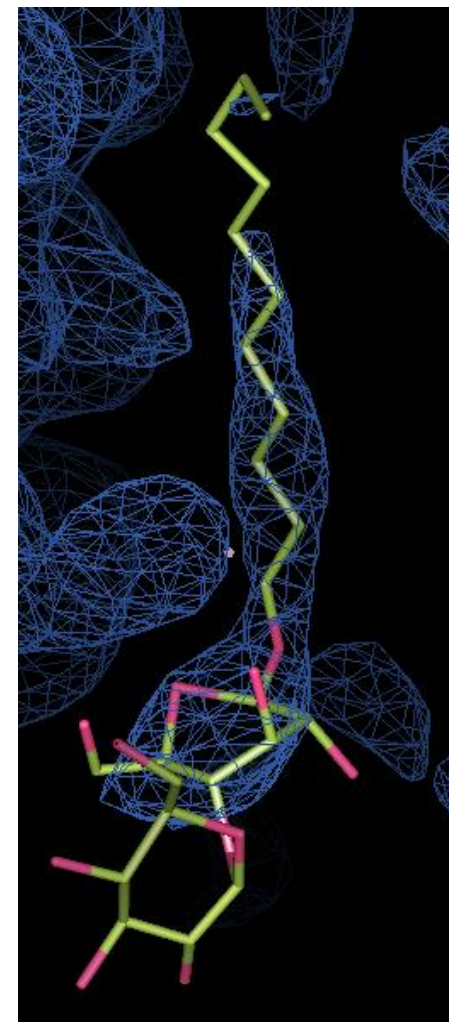
M. SQDG



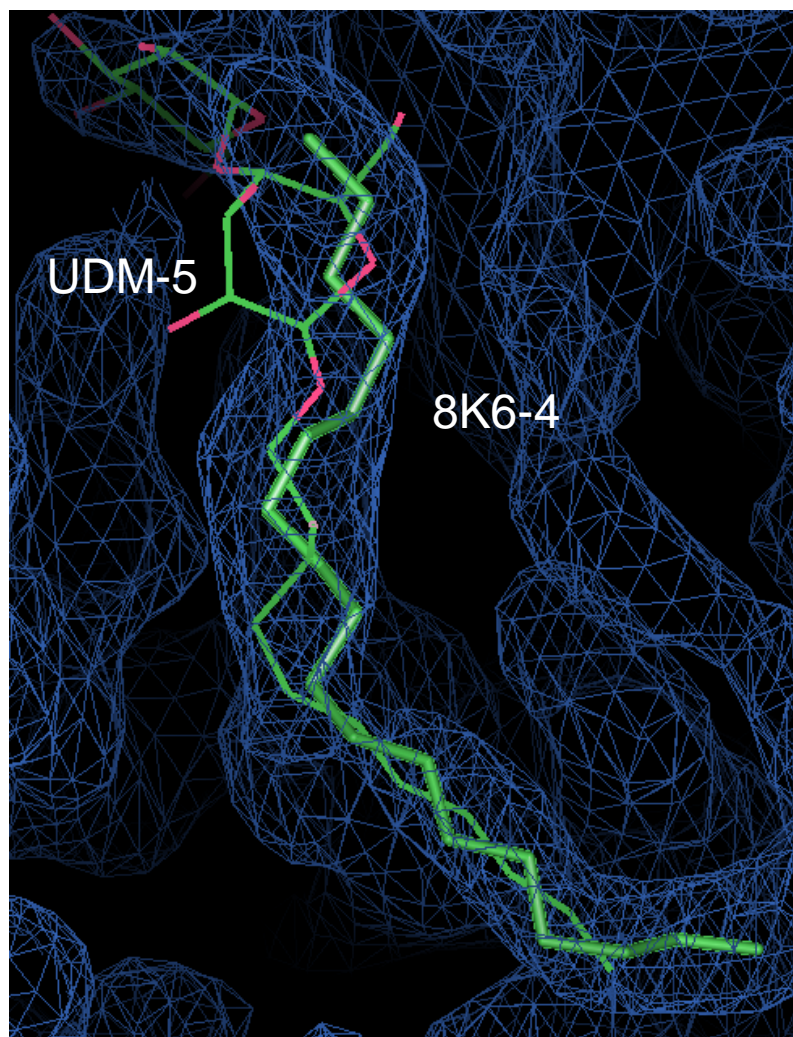
N. DAG9



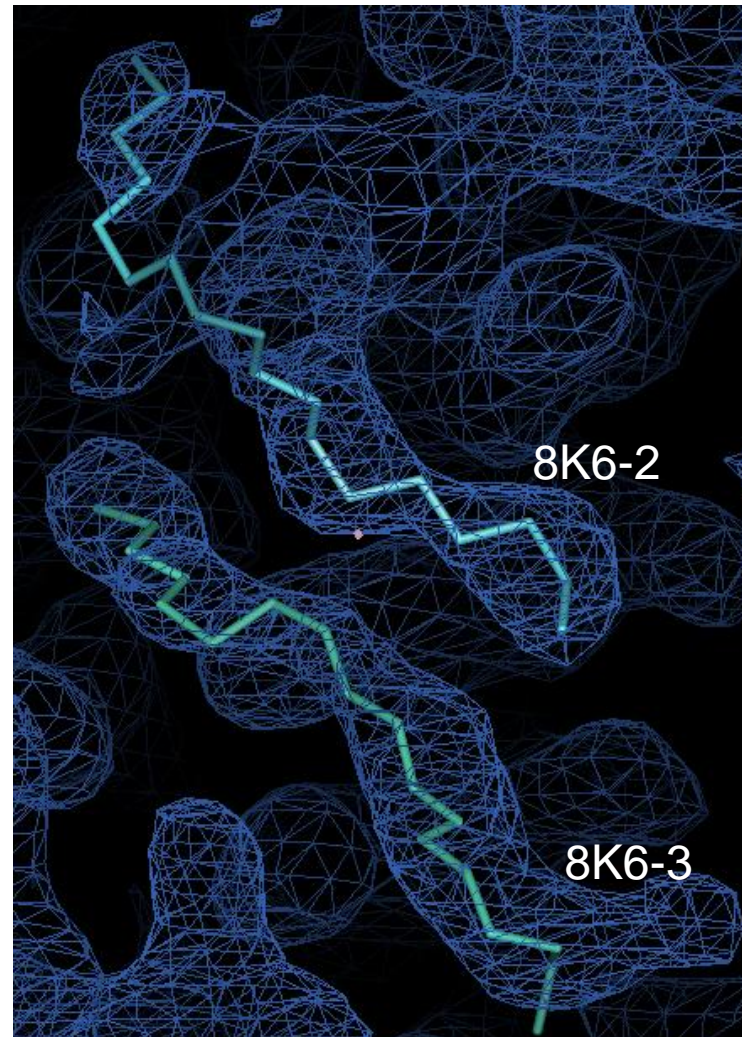
O. UDM1



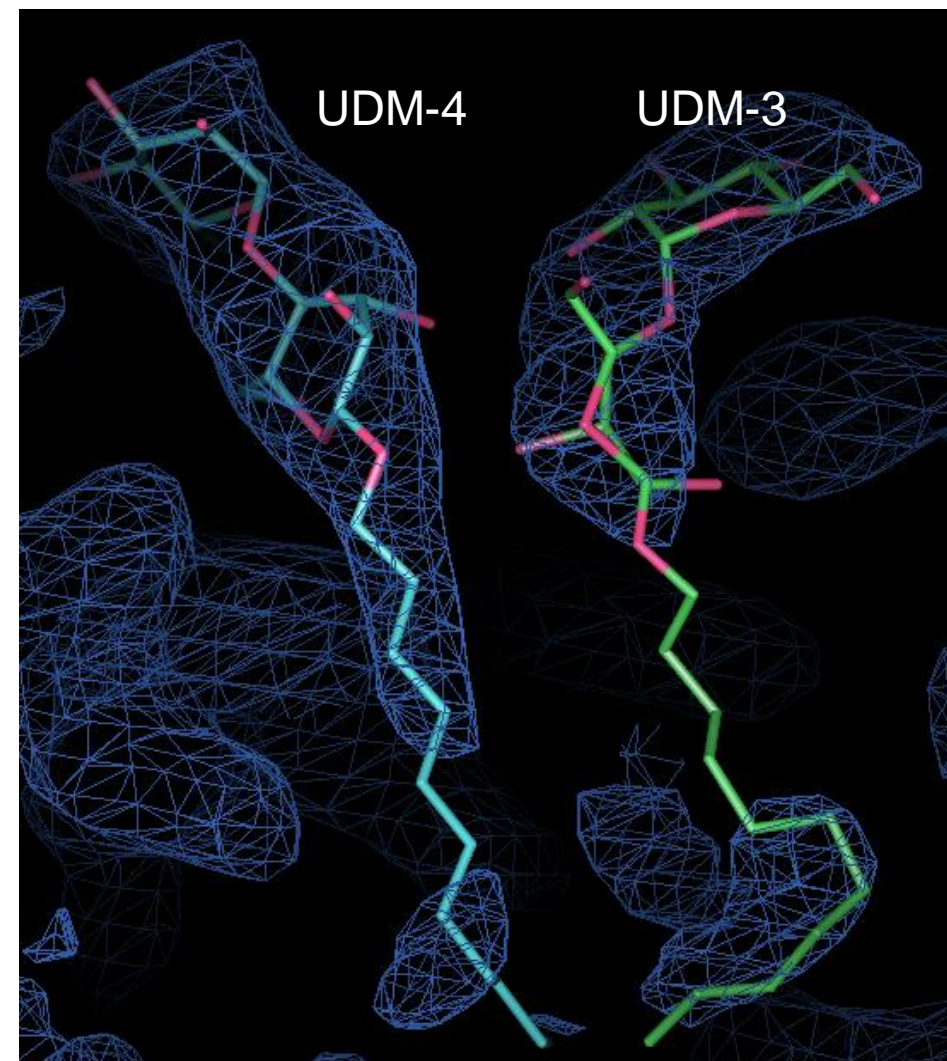
P. UDM5 and 8K6-4



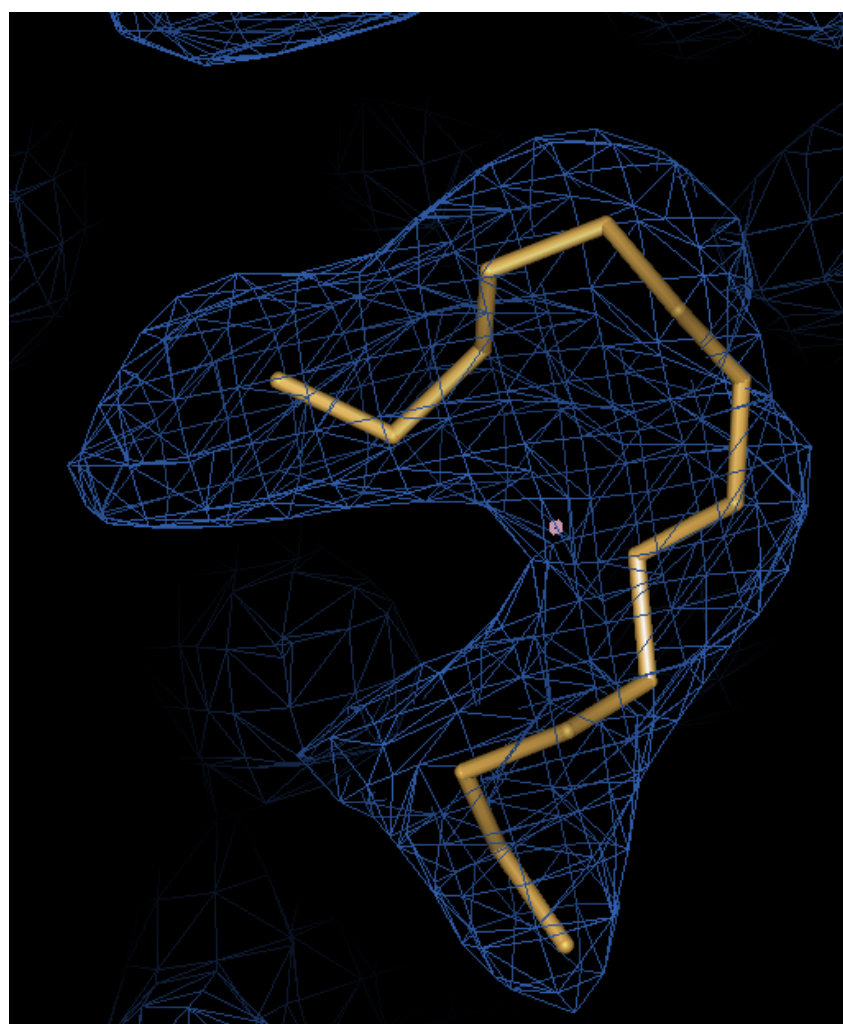
Q. 8K6-2 and 8K6-3



R. UDM3 and UDM4



S. 8K6-1



T. MYS

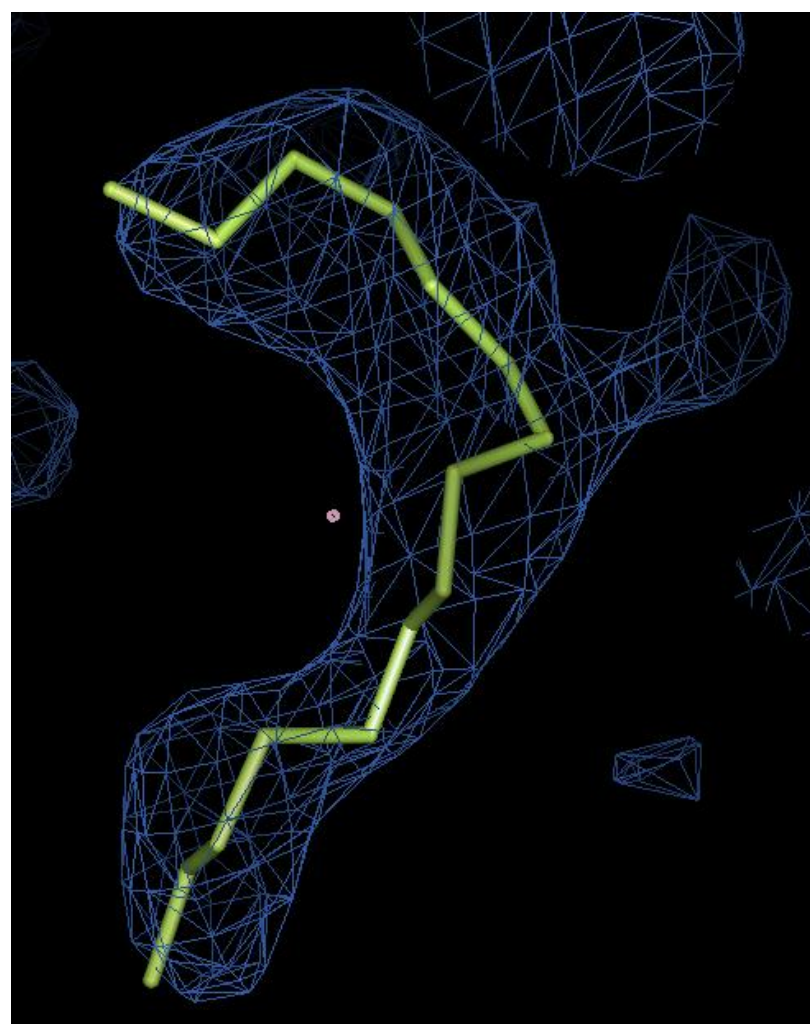


Figure S2

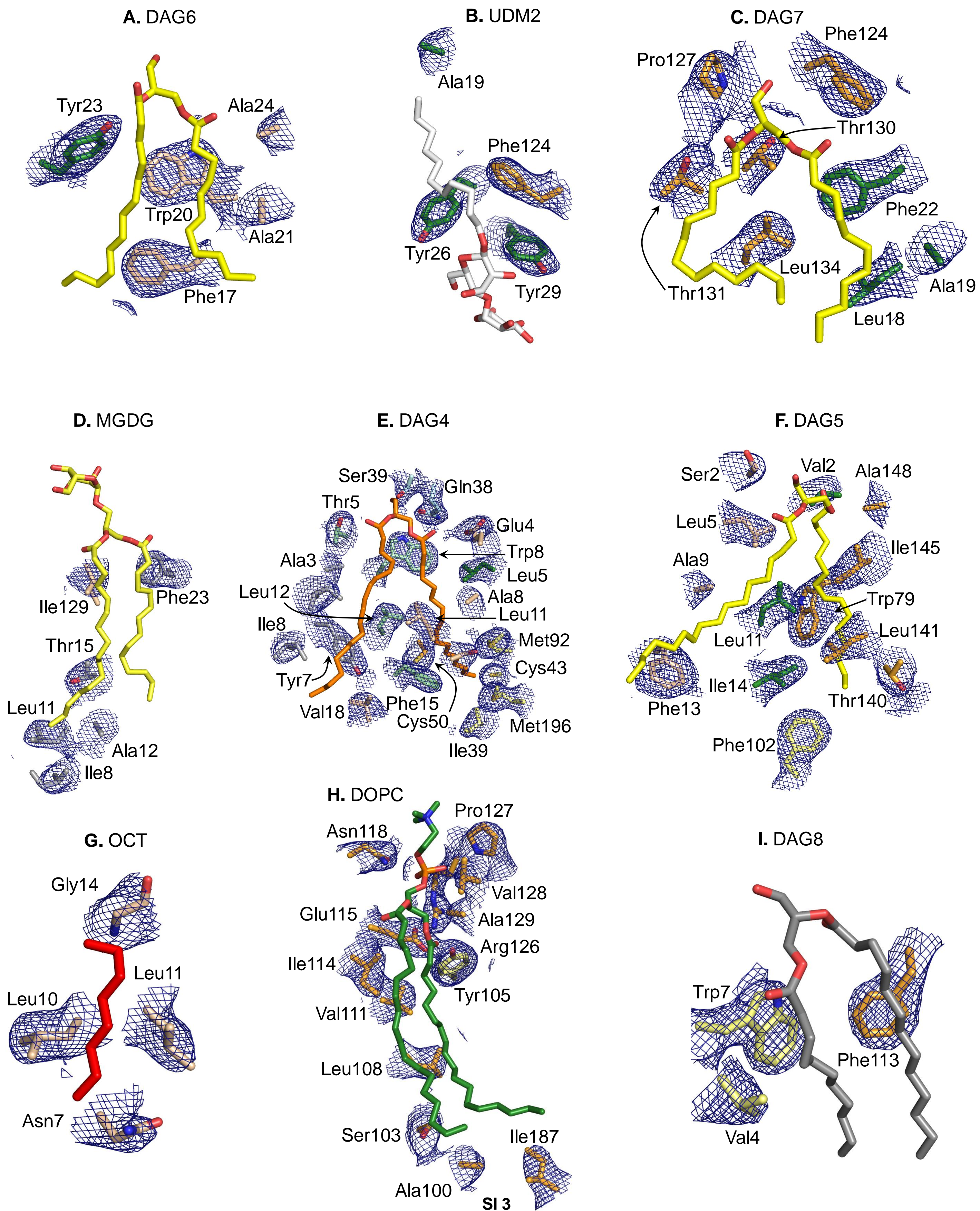
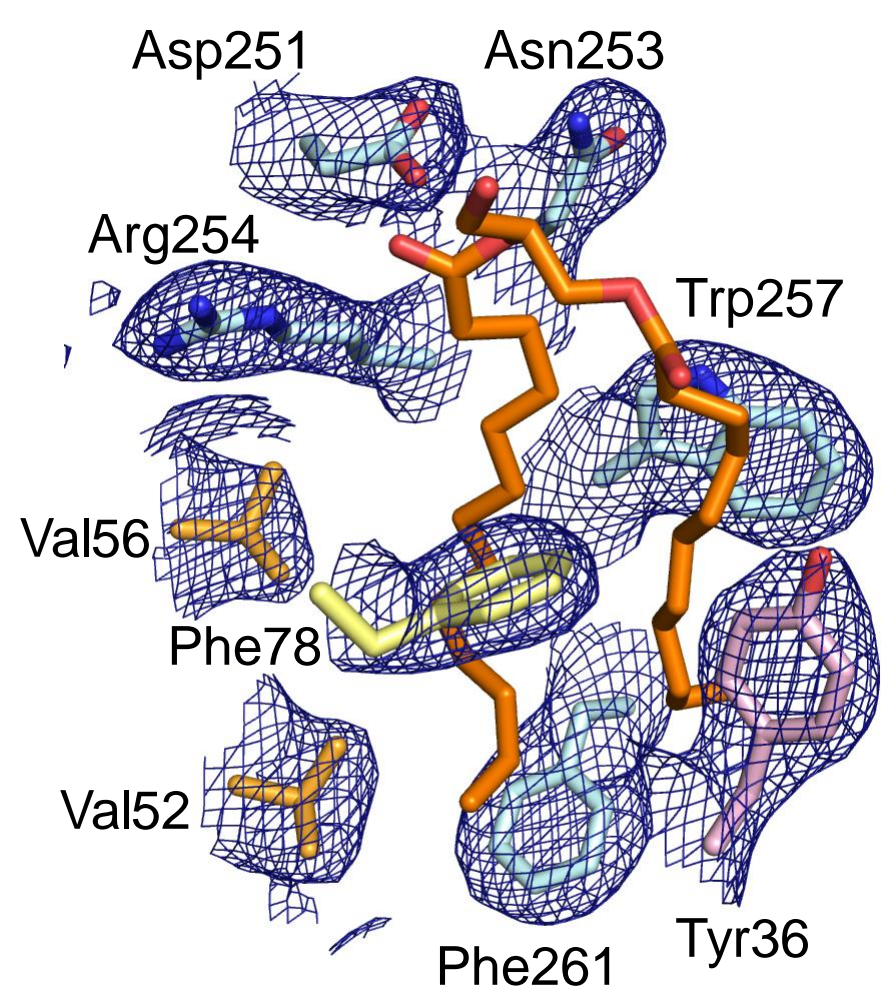
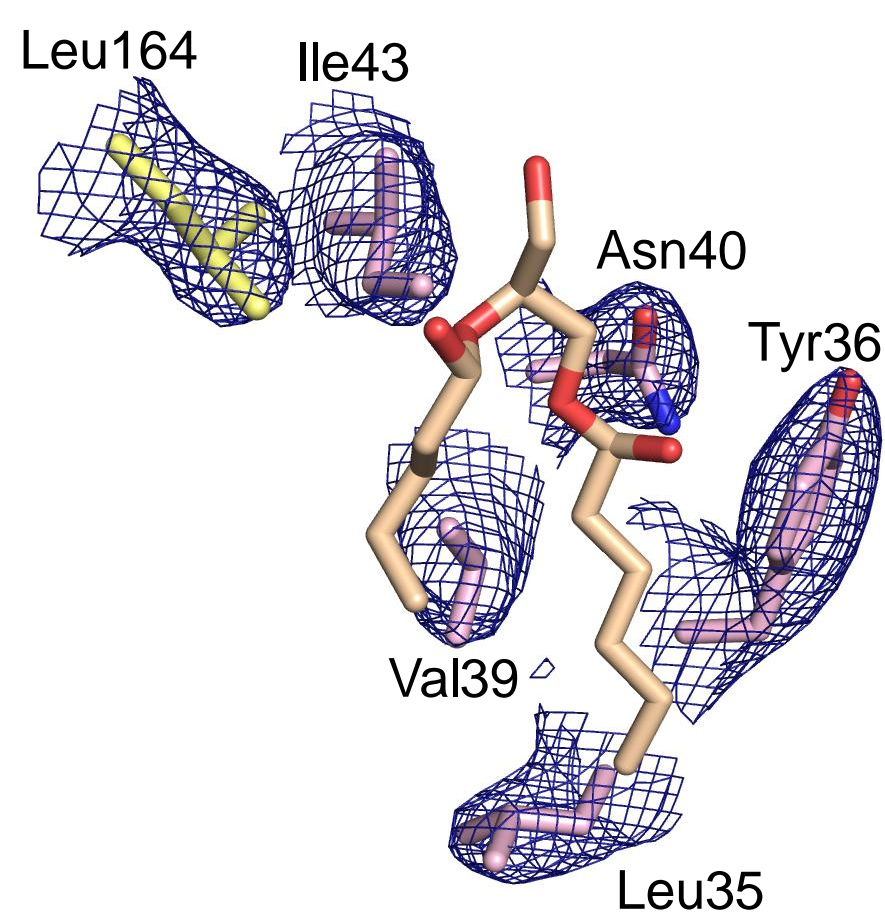


Figure S2

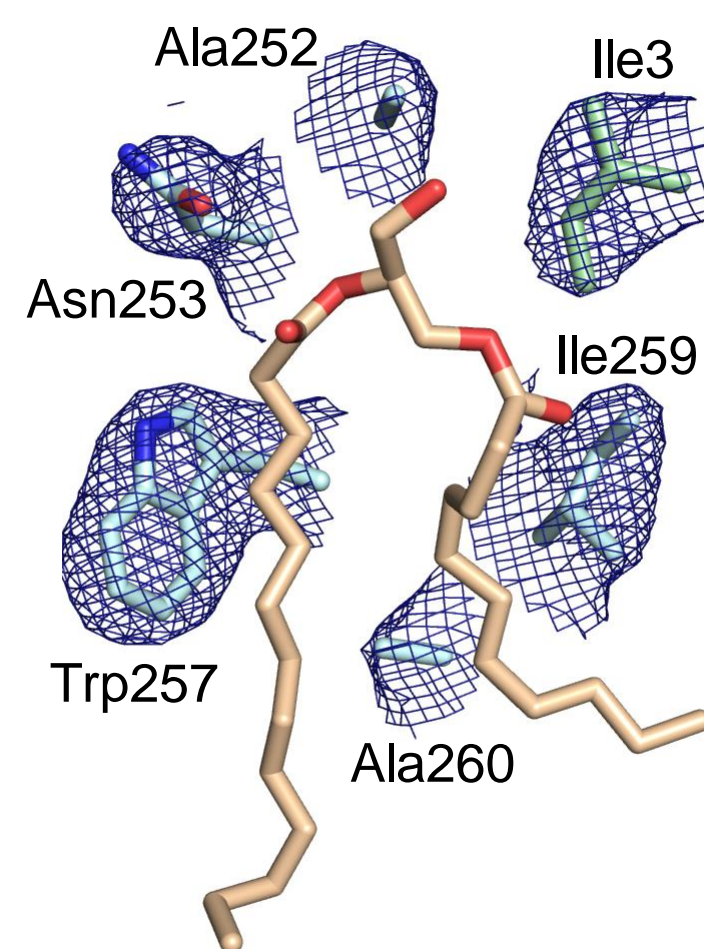
J. DAG2



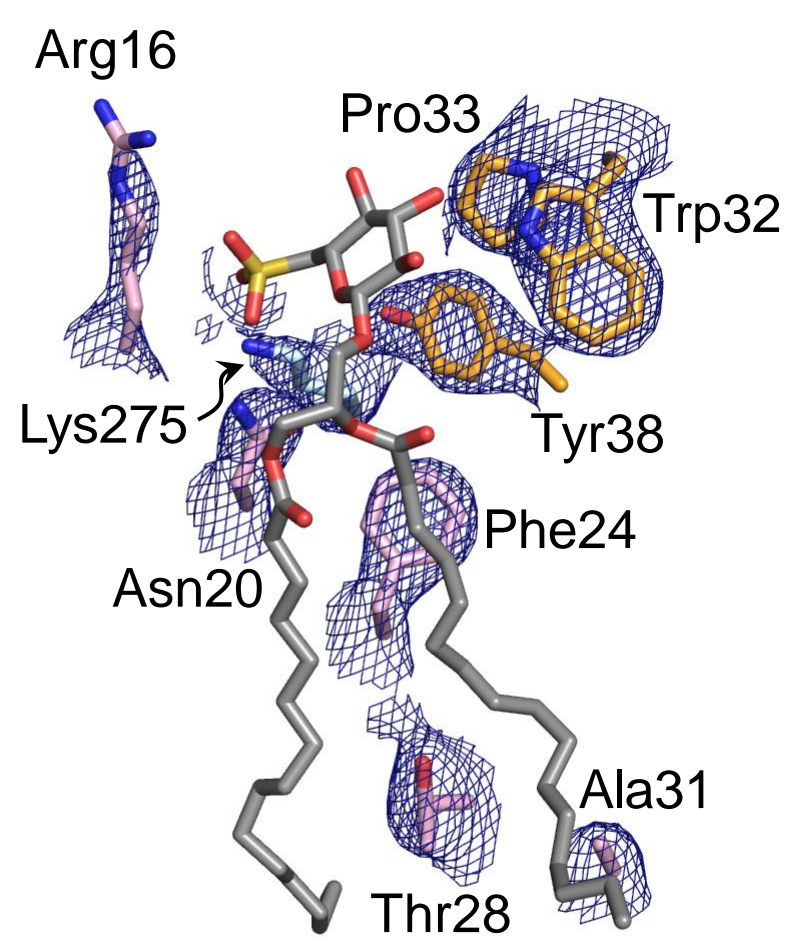
K. DAG1



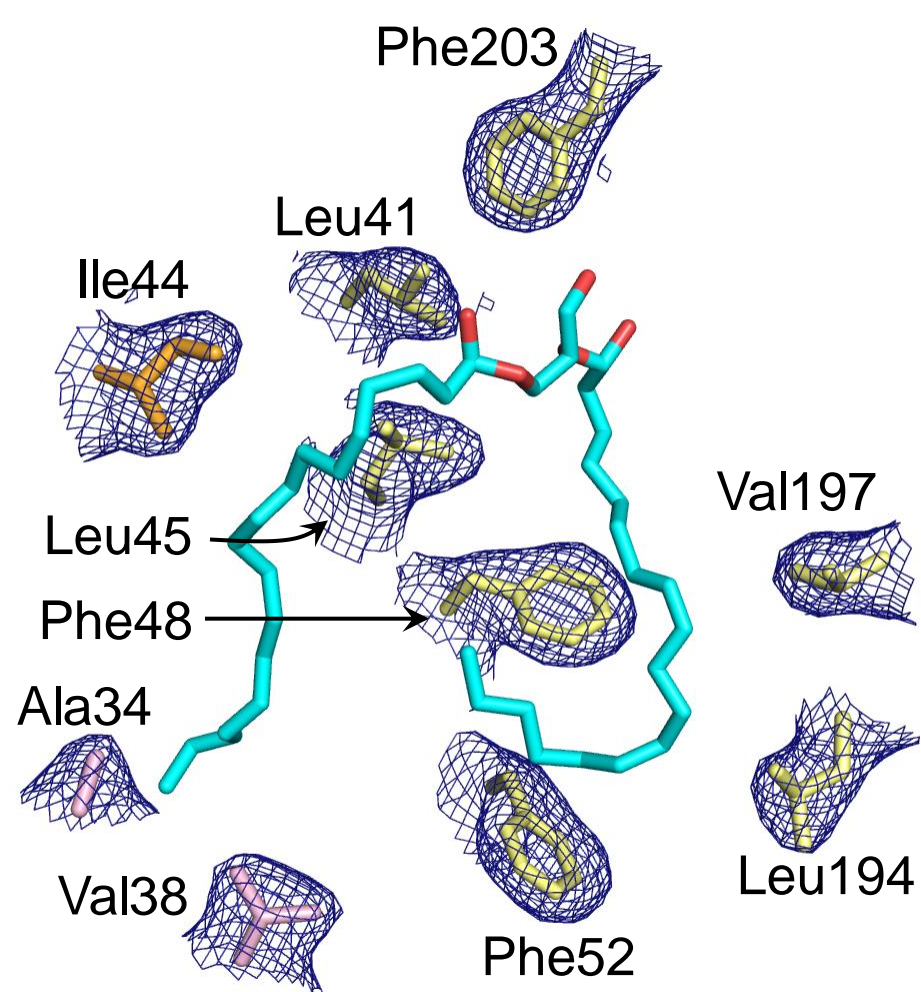
L. DAG3



M. SQDG



N. DAG9



O. UDM1

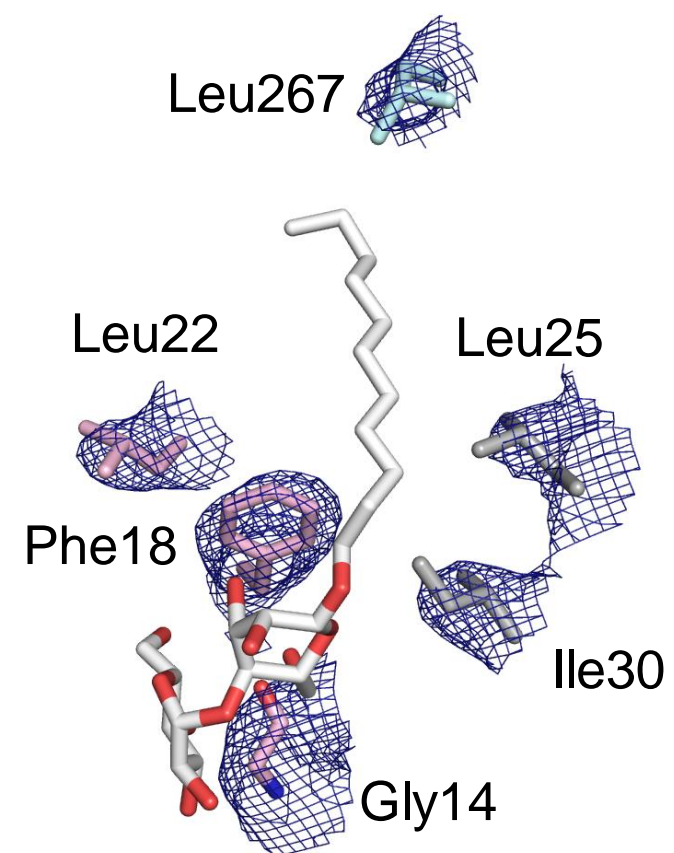
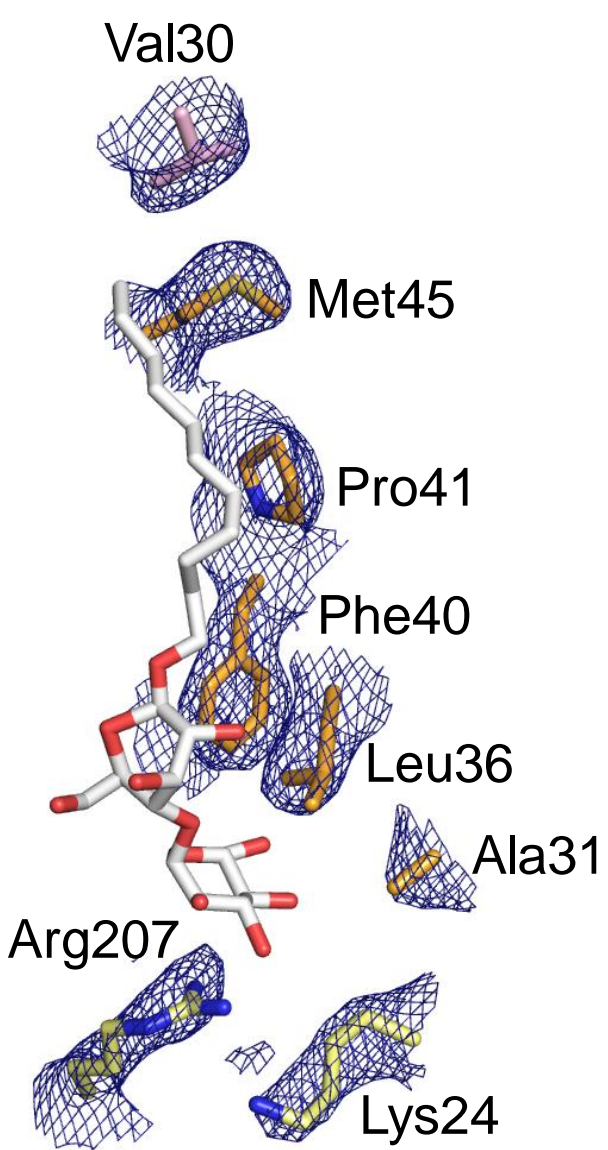
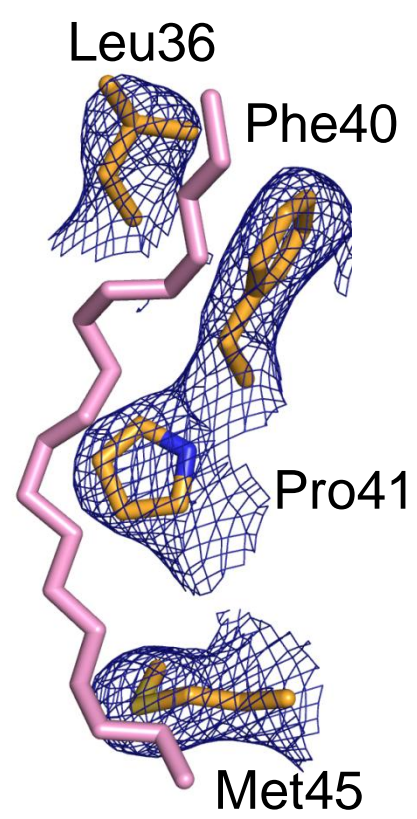


Figure S2

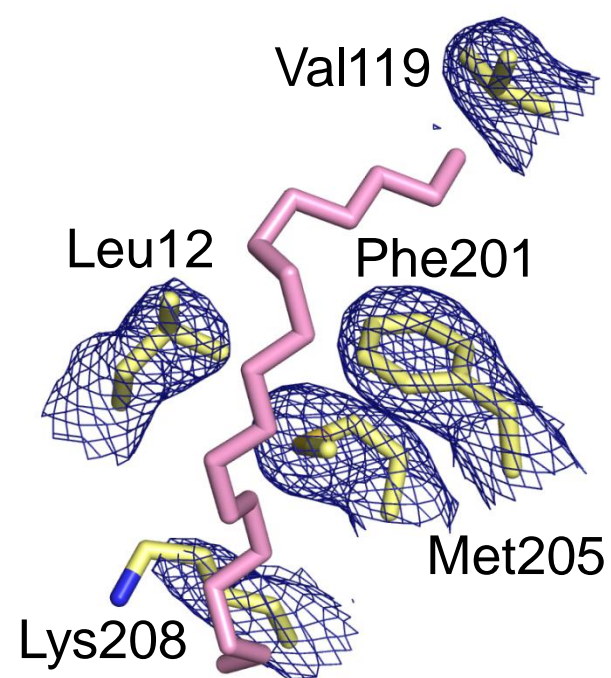
P(i). UDM5



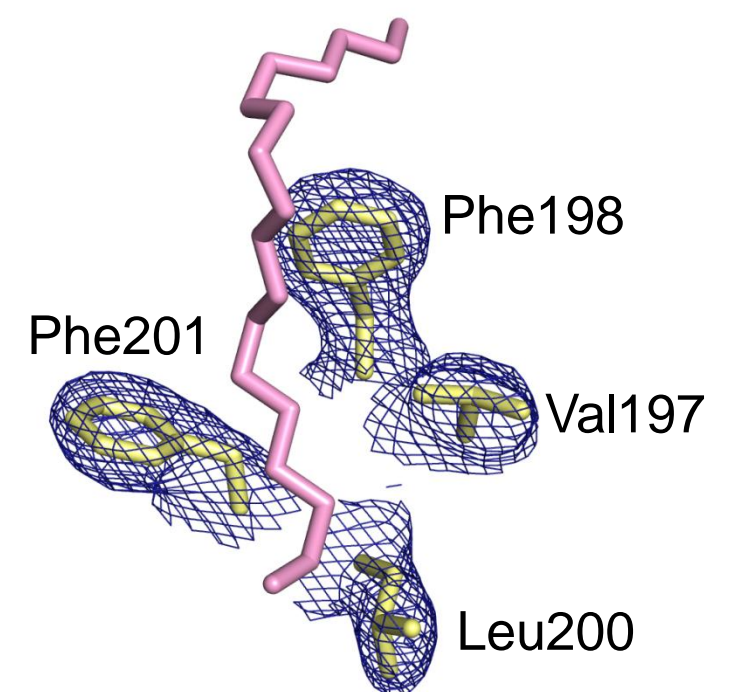
P(ii). 8K6-4



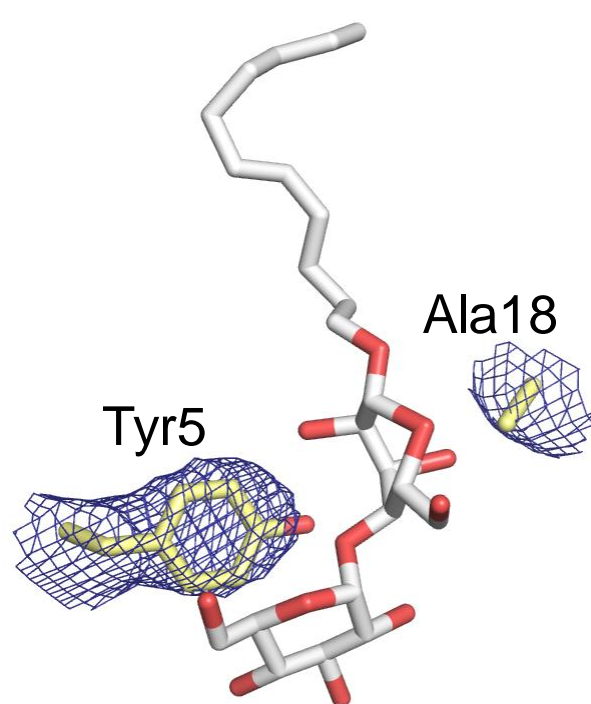
Q(i). 8K6-2



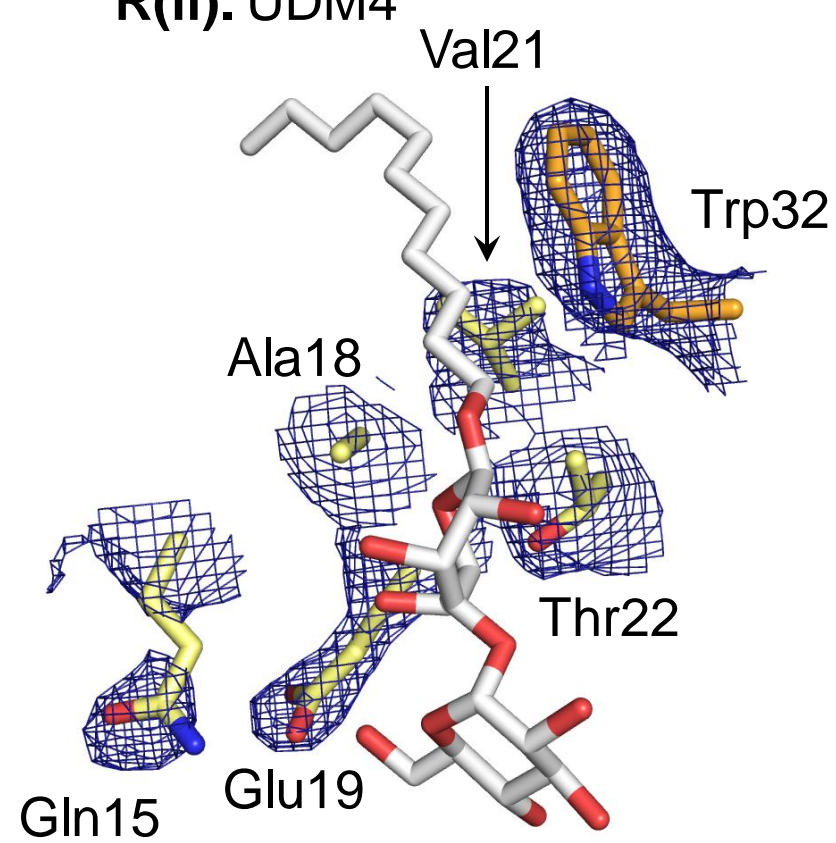
Q(ii). 8K6-3



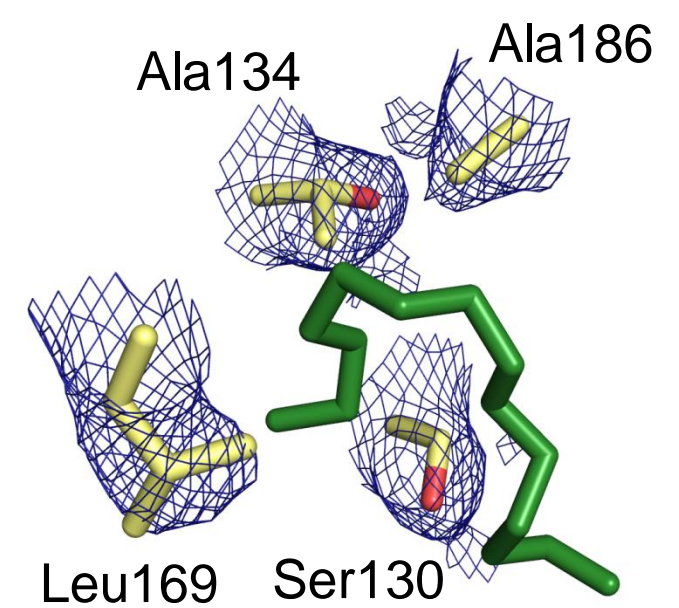
R(i). UDM3



R(ii). UDM4



S. 8K6-1



T. MYS

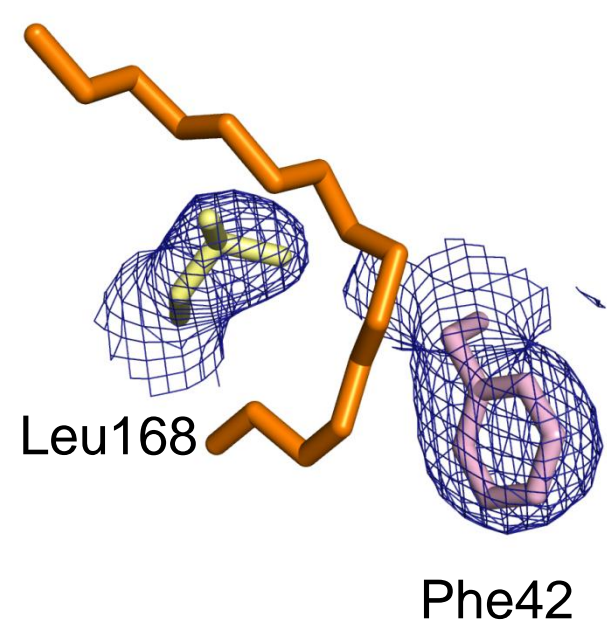
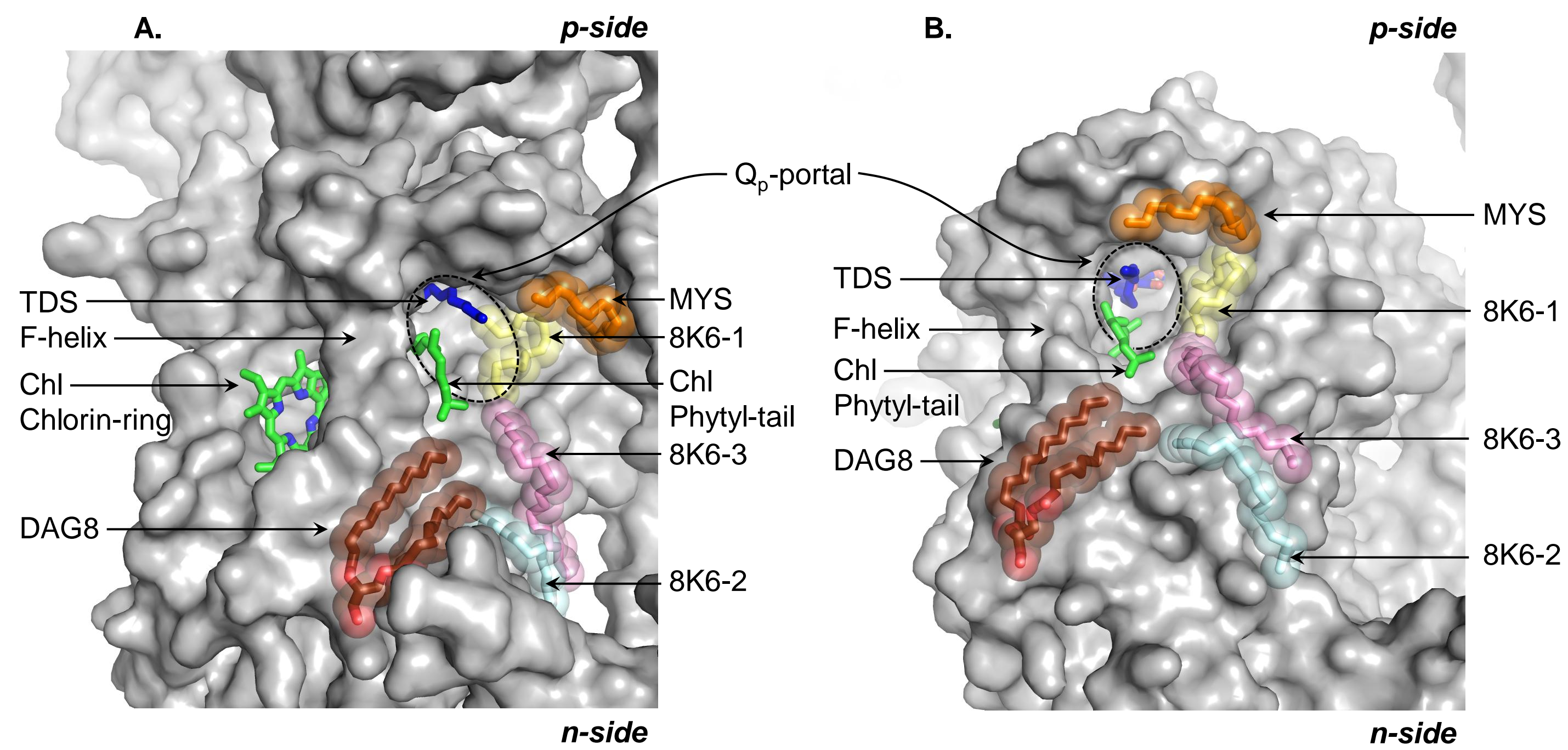


Figure S3



SUPPLEMENTAL INFORMATION

Supplemental Figure Legends

Figure S1 (Related to Figures 2, 3, and 4). Electron density (2Fo-Fc map, 1.0 σ) of lipids, a detergent, and a partially ordered acyl tail located proximal to the β -carotene. (A) DAG6, (B) UDM2, (C) DAG7, (D) MGDG, (E) DAG4, (F) DAG5, (G) OCT, (H) DOPC, (I) DAG8, (J) DAG2, (K) DAG1, (L) DAG3, (M) SQDG, (N) DAG9, (O) UDM1, (P) 8K6-4 and UDM5, (Q) 8K6-2 and 8K6-3, (R) UDM3 and UDM4, (S) 8K6-1, and, (T) MYS.

Figure S2 (Related to Figures 2, 3, and 4). Electron density (2Fo-Fc map, 1.2 σ) of amino acid residues forming binding sites of, (A) DAG6, (B) UDM2, (C) DAG7, (D) MGDG, (E) DAG4, (F) DAG5, (G) OCT, (H) DOPC, (I) DAG8, (J) DAG2, (K) DAG1, (L) DAG3, (M) SQDG, (N) DAG9, (O) UDM1, (P (i)) UDM5, (P (ii)) 8K6-4, (Q (i)) 8K6-2, (Q (ii)) 8K6-3, (R (i)) UDM3, (R (ii)) UDM4, (S) 8K6-1, and, (T) MYS. For details of polypeptide subunits, see **Supplemental Information Table T3**.

Figure S3 (Related to Figure 4). Lipidic environment in proximity of the Q_p -portal. Panels (A) and (B) show alternate views of the Q_p -portal entrance (highlighted with broken lines). The chlorophyll phytyl-tail (green sticks) penetrated the Q_p -portal. The quinone analog/inhibitor tridecyl-stigmatellin (TDS, shown as blue sticks; coordinates extracted from the b_6f complex structure PDB ID 2E76) is shown to mark the Q_p -portal. The lipid DAG8, and the alkyl chains MYS (15-carbons), 8K6-1, 8K6-2, and 8K6-3 (18-carbons), occupy the pathway connecting the Q_p -portal with the inter-monomer cavity.

Table T1 (Related to Figures 2, 3, and 4). Lipid Sites in Energy-Transducing Hetero-Oligomeric Membrane Protein Complexes. The table lists all the published cytochrome *b₆f* complex crystal structures, and provides details of the related cytochrome *bc₁* complex, NADH dehydrogenase complex (Ndh), cytochrome *c* oxidase (Cco), and photosystems II and I (PSII and I) for comparison. The cytochrome *b₆f* complex described in the present study is highlighted in blue.

Complex	PDB ID	d_{min} (Å) ¹	Oligomeric State	Polypeptides (per monomer) ²	Molecular Weight (kDa, assembly)	Lipid Sites (per monomer) ³
<i>b₆f</i>	4OGQ	2.50	Dimer	8	220	23
<i>b₆f</i>	1VF5 ⁽¹⁾	3.00	Dimer	8	220	2
<i>b₆f</i>	1Q90 ⁽²⁾	3.10	Dimer	8	220	4
<i>b₆f</i>	2D2C ⁽³⁾	3.80	Dimer	8	220	2
<i>b₆f</i>	2E74 ⁽⁴⁾	3.00	Dimer	8	220	7
<i>b₆f</i>	2E75 ⁽⁴⁾	3.55	Dimer	8	220	7
<i>b₆f</i>	2E76 ⁽⁴⁾	3.41	Dimer	8	220	7
<i>b₆f</i>	2ZT9 ⁽⁵⁾	3.00	Dimer	8	220	6
<i>b₆f</i>	4H44 ⁽⁶⁾	2.70	Dimer	8	220	12
<i>b₆f</i>	4H13 ⁽⁶⁾	3.07	Dimer	8	220	9
<i>b₆f</i>	4H0L ⁽⁶⁾	3.25	Dimer	8	220	7
<i>b₆f</i>	4I7Z ⁽⁷⁾	2.80	Dimer	8	220	10
<i>bc₁</i>	1KB9 ⁽⁸⁾	2.30	Dimer	10	360	6
<i>bc₁</i>	3CX5 ⁽⁹⁾	1.90	Dimer	10	360	6.5
Ndh	3RKO ⁽¹⁰⁾	3.00	Monomer	6	550	10
Cco	2GSM ⁽¹¹⁾	2.00	Monomer	2	100	11
Cco	3DTU ⁽¹²⁾	2.15	Monomer	2	100	23
Cco	3S8G ⁽¹³⁾	1.80	Monomer	3	80	20
Cco	2DYR ⁽¹⁴⁾	1.80	Dimer	13	400	19
PSII	3BZ2 ⁽¹⁵⁾	2.90	Dimer	20	550	32
PSII	3ARC ⁽¹⁶⁾	1.90	Dimer	19	550	56
PSI	1JB0 ⁽¹⁷⁾	2.50	Trimer	12	1000	4

¹ d_{min} , highest reported resolution; ²From crystal structure, without F_{ab}-fragments (PDB IDs 1KB9, 3CX5) and cytochrome *c* (PDB ID 3CX5); ³Including lipids, detergents and poly-carbon alkyl chains, with complete as well as partial crystallographic order.

Table T2 (Related to Figures 2, 3, and 4). Lipids, Detergents, and Acyl Chains Associated with the Cytochrome b_6f Complex Monomer. First column: (*Lipid/Detergent/Acyl Chain*) lists symbols used in the present study for lipidic molecules; second column (*Residue ID*): residue codes and IDs for each lipidic molecule in the PDB file; third column (*Sidedness (n or p)*) describes the location of lipidic molecules; fourth column (*Location (Boundary or Cavity)*): lipidic sites are classified into two groups, boundary or cavity, based on location; fifth column (*Lipid-Associated Trans-Membrane Helices*) lists protein segments within the interaction distance (4.0 Å) of each lipidic site.

Abbreviations- Cyt, cytochrome; ISP, Rieske iron-sulfur protein; SubIV, subunit IV; TMH, trans-membrane helix.

<i>Lipid/Detergent/Acyl Chain</i>	<i>Residue ID</i>	<i>Sidedness (n or p)</i>	<i>Location (Boundary or Cavity)</i>	<i>Lipid-Associated Trans-Membrane Helices</i>
DAG1	2WD (D206)	p	Boundary	ISP, <i>cd</i> -loop (cyt b_6)
DAG2	7PH (D203)	p	Boundary	Cyt <i>f</i> , ISP, E-TMH (subIV)
DAG3	7PH (C303)	p	Boundary	Cyt <i>f</i> , PetN
DAG4	3WM (E101)	p	Boundary	A, B-TMH (cyt b_6), E-TMH (subIV), PetL, PetM, PetG and PetN
DAG5	2WA (F101)	p	Boundary	B-TMH (cyt b_6), <i>ef</i> -loop and G-TMH (subIV), PetM, PetG
8-carbon chain (OCT)	OCT (F102)	p	Boundary	PetM
10-carbon chain (MYS)	MYS (D202)	p	Cavity	ISP, <i>cd</i> -loop (cyt b_6)
18-carbon chain (8K6-1)	8K6 (A308)	p	Cavity	C, D-TMH, <i>cd</i> -loop (cyt b_6),
DOPC	OPC (B204)	n	Boundary	F, G-TMH (subIV)
MGDG	1O2 (F103)	n	Boundary	PetL, PetM
DAG6	7PH (F104)	n	Boundary	PetM, PetG

DAG7	7PH (B205)	n	Boundary	G-TMH (subIV), PetG
UDM1	UMQ (D201)	n	Boundary	Cyt <i>f</i> , ISP, PetL
UDM2	UMQ (G101)	n	Boundary	<i>fg</i> -loop (subIV), PetG
UDM3	UMQ (A304)	n	Boundary/ Cavity	N-terminal surface helix (cyt <i>b</i> ₆)
UDM4	UMQ (B201)	n	Boundary/ Cavity	N-terminal surface helix (cyt <i>b</i> ₆), E-TMH (subIV)
18-carbon chain (8K6-2)	8K6 (A307)	n	Boundary/ Cavity	C, D-TMH (cyt <i>b</i> ₆)
18-carbon chain (8K6-3)	8K6 (A306)	n	Boundary/ Cavity	C, D-TMH (cyt <i>b</i> ₆)
DAG8	7PH (A305)	n	Boundary/ Cavity	N-terminal TMH, C-TMH (cyt <i>b</i> ₆), F-TMH (subIV)
SQDG	SQD (D204)	n	Cavity	Cyt <i>f</i> , ISP
DAG9	2WM (A309)	n	Cavity	A, D-TMH (cyt <i>b</i> ₆), E-TMH (subIV), ISP
UDM5	UMQ (B202)	n	Cavity	A, D-TMH (cyt <i>b</i> ₆), E-TMH (subIV)
18-carbon chain (8K6-4)	8K6 (B202)	n	Cavity	E-TMH (subIV)

Table T3 (Related to Figures 2, 3, and 4). Residues Forming Lipidic-Sites (within 4.0 Å). The residue code for each lipid/lipid-like molecule in the PDB file is provided in parenthesis.

Detergents-

1. UDM1 (UMQ, D201)-

Cytochrome *f* (chain C)- L267

Iron sulfur protein (chain D)- G14, F18, L22

PetL (chain E)- L25, I30

2. UDM2 (UMQ, G101)-

Subunit IV (chain B)- F124

PetG (chain G)- A19, Y26, Y29

3. UDM3 (UMQ, A304)-

Cytochrome *b*₆ (chain A)- Y5, A18

4. UDM4 (UMQ, B201)-

Cytochrome *b*₆ (chain A)- Q15, A18, E19, V21, T22

Subunit IV (chain B)- W32

5. UDM5 (UMQ, B202)-

Cytochrome *b*₆ (chain A)- K24, R207

Subunit IV (chain B)- A31, L36, F40, P41, M45

Iron-sulfur protein (chain D)- V30

Lipids-

6. DAG1 (2WD, D206)-

Cytochrome *b*₆ (chain A)- L164

Iron-sulfur protein (chain D)- L35, Y36, V39, N40, I43

7. DAG2 (7PH, D203)-

Cytochrome b_6 (chain A)- F78

Subunit IV (chain B)- V52, V56

Cytochrome f (chain C)- D251, N253, R254, W257, F261

Iron-sulfur protein (chain D)- G33, Y36

8. DAG3 (7PH, C303)-

Cytochrome f (chain C)- A252, N253, G256, W257, I259, A260

PetN (chain H)- I3

9. DAG4 (3WM, E101)-

Cytochrome b_6 (chain A)- I39, C43, M92, M96

Subunit IV (chain B)- C50

Cytochrome f (chain C)- Q38, S39

PetL (chain E)- A3, I4, Y7, I8

PetM (chain F)- E4, A8, L11, S12, V18

PetG (chain G)- L5

PetN (chain H)- T5, W8, L12, F15

10. DAG5 (2WA, F101)-

Cytochrome b_6 (chain A)- F102

Subunit IV (chain B)- W79, T140, L141, G144, I145, A148

PetM (chain F)- S2, L5, A9, F13

PetG (chain G)- V2, L11, I14

11. DAG6 (7PH, F104)-

PetM (chain F)- F17, W20, A21, A24

PetG (chain G)- Y23

12. DAG7 (7PH, B205)-

Subunit IV (chain B)- F124, P127, T130, T131, L134

PetG (chain G)- L18, A19, F22

13. DAG8 (7PH, A305)-

Cytochrome b_6 (chain A)- V4, W7

Subunit IV (chain B)- F113

14. DAG9 (2WM, A309)-

Cytochrome b_6 (chain A)- L41, L45, F48, F52, L194, V197, F203

Subunit IV (chain B)- I44

Iron-sulfur protein (chain D)- A34, V38

15. MGDG (1O2, F103)-

PetL (chain E)- I8, L11, A12, T15, G16, F23

PetM (chain F)- K28, I29, G31

16. SQDG (SQD, D204)-

Subunit IV (chain B)- W32, P33, Y38

Cytochrome f (chain C)- K275

Iron-sulfur protein (chain D)- R16, N20, F24, G25, T28, G29, A31

17. DOPC (OPC, B204)-

Cytochrome b_6 (chain A)- Y105

Subunit IV (chain B)- I87, A100, S103, G107, L108, V111, I114, E115, N118, R126, P127, V128, A129

Acyl chains-

18. 8K6-1 (8K6, A308)-

Cytochrome b_6 (chain A)- S130, T134, L169, A186

19. 8K6-2 (8K6, A307)-

Cytochrome b_6 (chain A)- L12, V119, F201, M205, K208

20. 8K6-3 (8K6, A306)-

Cytochrome b_6 (chain A)- V197, F198, L200, F201

21. 8K6-4 (8K6, B202)-

Subunit IV (chain B)- L36, F40, P41, M45

22. MYS (MYS, D202)-

Cytochrome b_6 (chain A)- L168

Iron-sulfur protein (chain D)- F42

23. OCT (OCT, F102)-

PetM (chain F)- N7, L10, L11, G14

Table T4 (Related to Figures 1, 2, 3, and 4). Lipid composition of thylakoid membranes (expressed as molar percentage).

Lipid	MGDG	DGDG	SQDG	PG
<i>Synechocystis</i> PCC 6803 ⁽¹⁸⁾	62	14	18	6
Spinach ⁽¹⁹⁾	45-50	25-30	10	10

Abbreviations: DGDG, digalactosyldiacylglycerol; MGDG, monogalactosyldiacylglycerol; PG, phosphatidylglycerol; SQDG, sulfoquinovosyldiacylglycerol.

Synechocystis PCC 6803 is a representative cyanobacterium, while spinach is a representative eukaryotic photosynthetic organism.

MGDG and DGDG are neutral lipids, while SQDG and PG are anionic lipids.

Table T5 (Related to Figure 1, 2, 3, and 4). Fatty acid composition of cyanobacterial thylakoid membranes ⁽¹⁸⁾.

Fatty Acid (molar %)*	<i>Synechocystis</i> PCC 6803	<i>Synechococcus</i> PCC 7002	<i>Anabaena</i> <i>variabilis</i>**	<i>Mastigocladus</i> <i>laminosus</i>
14:0	Trace	1	0	1
14:1 (9)	0	0	0	0
16:0	51	35	29	19
16:1 (9)	3	19	22	50
16:2 (9, 12)	0	0	3	0
18:0	Trace	Trace	Trace	1
18:1 (9)	2	10	7	27
18:2 (9, 12)	6	25	15	0
18:3 (9, 12, 15)	8	10	24	0
18:3 (6, 9, 12)	21	0	0	0
18:4 (6, 9, 12, 15)	8	0	0	0

*Fatty acids are represented as- length of carbon chain:number of double bonds (position(s) of double bond(s)); ***Anabaena variabilis* is related to *Nostoc* PCC 7120, the source organism for the cytochrome *b₆f* complex protein crystallized in the present study; *Synechocystis* PCC 6803 and *Synechococcus* PCC 7002 are unicellular cyanobacteria while *Anabaena variabilis* and *Mastigocladus laminosus* are filamentous strains.

SUPPLEMENTAL REFERENCES

1. Kurisu, G., Zhang, H., Smith, J. L., and Cramer, W. A. (2003) Structure of the cytochrome b_6f complex of oxygenic photosynthesis: Tuning the cavity, *Science* 302, 1009-1014.
2. Stroebel, D., Choquet, Y., Popot, J. L., and Picot, D. (2003) An atypical haem in the cytochrome b_6f complex, *Nature* 426, 413-418.
3. Yan, J., Kurisu, G., and Cramer, W. A. (2006) Intraprotein transfer of the quinone analogue inhibitor 2,5-dibromo-3-methyl-6-isopropyl-p-benzoquinone in the cytochrome b_6f complex, *Proc Natl Acad Sci U. S. A.* 103, 69-74.
4. Yamashita, E., Zhang, H., and Cramer, W. A. (2007) Structure of the cytochrome b_6f complex: quinone analogue inhibitors as ligands of heme c_n , *J Mol Biol* 370, 39-52.
5. Baniulis, D., Yamashita, E., Whitelegge, J. P., Zatsman, A. I., Hendrich, M. P., Hasan, S. S., Ryan, C. M., and Cramer, W. A. (2009) Structure-function, stability, and chemical modification of the cyanobacterial cytochrome b_6f complex from *Nostoc* sp. PCC 7120, *J Biol Chem* 284, 9861-9869.
6. Hasan, S. S., Yamashita, E., Baniulis, D., and Cramer, W. A. (2013) Quinone-dependent proton transfer pathways in the photosynthetic cytochrome b_6f complex, *Proc Natl Acad Sci U.S.A.* 110, 4297-4302.
7. Hasan, S. S., Stofleth, J. T., Yamashita, E., and Cramer, W. A. (2013) Lipid-induced conformational changes within the cytochrome b_6f complex of oxygenic photosynthesis, *Biochemistry* 52, 2649-2654.
8. Lange, C., Nett, J. H., Trumpower, B. L., and Hunte, C. (2001) Specific roles of protein-phospholipid interactions in the yeast cytochrome bc_1 complex structure, *EMBO J* 20, 6591-6600.
9. Solmaz, S. R., and Hunte, C. (2008) Structure of complex III with bound cytochrome c in reduced state and definition of a minimal core interface for electron transfer, *J Biol Chem* 283, 17542-17549.

10. Efremov, R. G., and Sazanov, L. A. (2011) Structure of the membrane domain of respiratory complex I, *Nature* 476, 414-420.
11. Qin, L., Hiser, C., Mulichak, A., Garavito, R. M., and Ferguson-Miller, S. (2006) Identification of conserved lipid/detergent-binding sites in a high-resolution structure of the membrane protein cytochrome *c* oxidase, *Proc Natl Acad Sci U. S. A.* 103, 16117-16122.
12. Qin, L., Mills, D. A., Buhrow, L., Hiser, C., and Ferguson-Miller, S. (2008) A conserved steroid binding site in cytochrome *c* oxidase, *Biochemistry* 47, 9931-9933.
13. Tiefenbrunn, T., Liu, W., Chen, Y., Katritch, V., Stout, C. D., Fee, J. A., and Cherezov, V. (2011) High resolution structure of the *ba*₃ cytochrome *c* oxidase from *Thermus thermophilus* in a lipidic environment, *PLoS ONE* 6, e22348.
14. Shinzawa-Itoh, K., Aoyama, H., Muramoto, K., Terada, H., Kurauchi, T., Tadehara, Y., Yamasaki, A., Sugimura, T., Kurono, S., Tsujimoto, K., Mizushima, T., Yamashita, E., Tsukihara, T., and Yoshikawa, S. (2007) Structures and physiological roles of 13 integral lipids of bovine heart cytochrome *c* oxidase, *EMBO J* 26, 1713-1725.
15. Guskov, A., Kern, J., Gabdulkhakov, A., Broser, M., Zouni, A., and Saenger, W. (2009) Cyanobacterial photosystem II at 2.9-Å resolution and the role of quinones, lipids, channels and chloride, *Nature Str Mol Biol* 16, 334-342.
16. Umena, Y., Kawakami, K., Shen, J. R., and Kamiya, N. (2011) Crystal structure of oxygen-evolving photosystem II at a resolution of 1.9 Å, *Nature* 473, 55-60.
17. Jordan, P., Fromme, P., Witt, H. T., Klukas, O., Saenger, W., and Krauss, N. (2001) Three-dimensional structure of cyanobacterial photosystem I at 2.5 Å resolution, *Nature* 411, 909-917.
18. Wada, H., and Murata, N. (1998) Membrane lipids in cyanobacteria, *Lipids Photosynth: Str Func Gen* (Eds. Siegenthaler, P. A., and Murata, N., Kluwer Academic Publishers) 6, 65-81.
19. Gounaris, K., Barber, J., and Harwood, J. L. (1986) The thylakoid membranes of higher plant chloroplasts, *Biochem J*, 237, 313-326.